

 Open access • Journal Article • DOI:10.1139/CJC-2015-0593

Thin flexible lithium-ion battery featuring graphite paper based current collectors with enhanced conductivity — [Source link](#)

Hang Qu, Jingshan Hou, Yufeng Tang, Oleg A. Semenikhin ...+1 more authors

Institutions: École Polytechnique de Montréal, Chinese Academy of Sciences, University of Western Ontario

Published on: 01 Feb 2017 - Canadian Journal of Chemistry (NRC Research Press)

Topics: Separator (electricity), Lithium-ion battery, Anode, Current collector and Cathode

Related papers:

- [Current Collectors for Flexible Lithium Ion Batteries: A Review of Materials](#)
- [Preparation and Electrochemical Properties of Si@C/Graphite Composite as Anode for Lithium-Ion Batteries](#)
- [Three-Dimensional Double-Walled Ultrathin Graphite Tube Conductive Scaffold with Encapsulated Germanium Nanoparticles as a High-Areal-Capacity and Cycle-Stable Anode for Lithium-Ion Batteries](#)
- [A long life 4 V class lithium-ion polymer battery with liquid-free polymer electrolyte](#)
- [N-Carbon from Waste Tea as Efficient Anode Electrode Material in Lithium Ion Batteries](#)

Share this paper:    

View more about this paper here: <https://typeset.io/papers/thin-flexible-lithium-ion-battery-featuring-graphite-paper-1g57o45uq8>



Canadian Journal of Chemistry
Revue canadienne de chimie

**Thin Flexible Lithium Ion Battery Featuring Graphite Paper
Based Current Collectors with Enhanced Conductivity**

Journal:	<i>Canadian Journal of Chemistry</i>
Manuscript ID	cjc-2015-0593.R1
Manuscript Type:	Article
Date Submitted by the Author:	09-Aug-2016
Complete List of Authors:	Qu, Hang; Ecole Polytechnique de Montreal Hou, Jingshan; Ecole Polytechnique de Montreal Tang, Yufeng; Shanghai Institute of Ceramics, Chinese Academy of Sciences, Semenikhin, Oleg; University of Western Ontario Skorobogatiy, Maksim; Ecole Polytechnique de Montreal
Keyword:	Lithium-ion batteries, Flexible batteries, Ultra-thin battery films, graphite paper current collectors

SCHOLARONE™
Manuscripts

Thin Flexible Lithium Ion Battery Featuring Graphite Paper Based Current Collectors with Enhanced Conductivity

Hang Qu¹, Jingshan Hou¹, Yufeng Tang², Oleg Semenikhin³, and Maksim Skorobogatiy^{1,*}

¹ Department of Physics Engineering, Ecole Polytechnique de Montreal, Montreal, Quebec,
H3C 3A7, Canada.

² CAS Key Laboratory of Materials for Energy Conversion, Shanghai Institute of Ceramics,
Chinese Academy of Sciences, Shanghai 200050, PR China.

³ Department of Chemistry, Western University, London, Ontario, N6A 5B7, Canada.

Draft

Abstract: A flexible, light weight and high conductivity current collector is the key element that enables fabrication of high performance flexible lithium ion battery. Here we report a thin, light weight and flexible lithium ion battery that uses graphite papers deposited with nano-sized metallic layers as the current collector, LiFePO_4 and $\text{Li}_4\text{Ti}_5\text{O}_{12}$ as the cathode and anode materials, and a PE membrane soaked in LiPF_6 as the separator. Using thin and flexible graphite paper as a substrate for the current collector instead of a rigid and heavy metal foil enables us to demonstrate an ultra-thin lithium-ion battery (total thickness including encapsulation layers of less than $250\ \mu\text{m}$) that also features light weight and high flexibility.

Key words: Lithium-ion batteries, flexible batteries, graphite paper current collectors

1 Introduction

Many wearable and portable electronic devices require efficient, compliant power sources that can fully function when bent, folded, or compressed. Lithium-ion batteries (LIBs) dominate the portable power-source market due to their high energy density, high output voltage, long-term stability and environmentally friendly operation.¹ High performance flexible LIBs are considered to be one of the most promising candidates of power sources for the next generation flexible electronic devices.¹⁻³ LIBs typically consist of several functional layers (see Fig. 1a). When battery flexibility is desired, all of the battery components should be flexible.¹ Among the various functional layers, the current collectors affect critically the battery performance, and their flexibility is typically difficult to achieve together with a high conductivity.

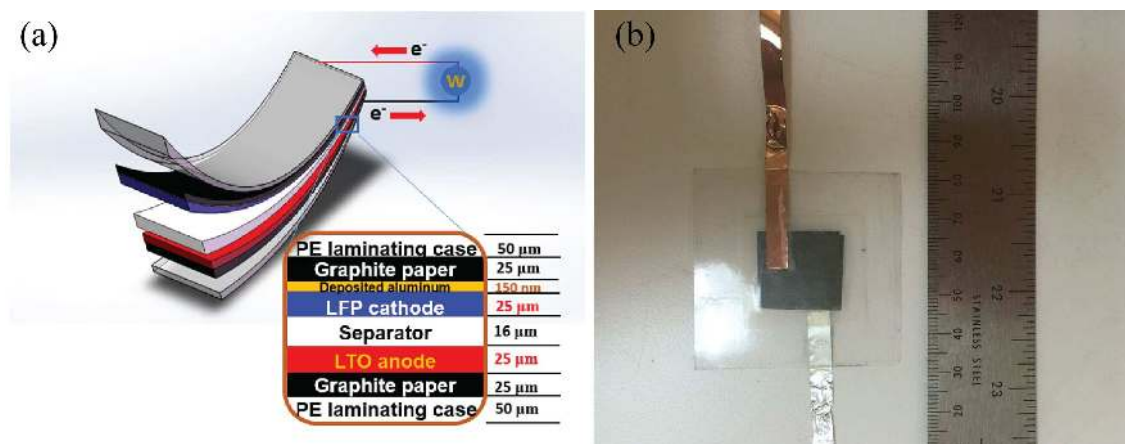


Fig.1 (a) Schematic of the thin, flexible lithium-ion battery; (b) A lithium-ion battery sample;

Many approaches have been explored for designing flexible LIBs.⁴⁻⁸ Traditionally, electrode active materials are coated onto a Cu foil which then works as anode, and an Al foil is generally used as cathode. The as-fabricated LIBs are typically heavy and rigid, which makes them unsuitable for truly wearable applications. Recently, tremendous effort has been dedicated to the R&D of LIBs that utilize thin flexible current collectors and free-standing electrodes. Among these studies, conductive films based on carbon nanotubes (CNTs) or CNT composites are popularly used as current collectors or binder-free electrodes due to their appealing electrical and mechanical properties such as high conductivity, high mechanical strength, and large activated surface areas. For example, Wang et al. reported a CNT current collector fabricated by cross-stacking continuous CNT films drawn from super-aligned CNT arrays.⁹ Flexible LIB electrode could be then deposited on the fabricated CNT films. Compared to metallic current collectors, CNT films exhibit a stronger adherence to battery materials. Besides, Sun et al. developed flexible nano-porous CNT films directly on a polypropylene separator using vacuum filtration technique.¹⁰ The as-fabricated CNT films

were utilized as binder-free and current collector-free anodes in LIBs. An electrochemical half-cell was fabricated using a CNT film as anode and a lithium-foil as counter electrode, and the specific capacity of the CNT film anode was measured to be ~ 380 mAh/g. Later the same group also fabricated an LIB electrode based on CNT/graphite-nanosheets (GN) composite films with an optimized CNT/GN ratio of 2:1.¹¹ The reversible capacity of the CNT/GN electrode was found to be 375 mAh/g. More recently, Yoon et al. synthesized CNT films via chemical vapor deposition followed by a direct spinning process.¹² The CNT films were then processed by a heating treatment to increase the crystalline perfection. Experimental results showed that the electrode based on heat-treated CNT films exhibited a higher capacity of ~ 446 mAh/g that was around twice as the case of the electrode based on raw CNT films. Though CNT films feature great electrochemical properties for LIB applications, the synthesis of CNT (or CNT-composite) films normally requires a sophisticated process, and cost of such materials is high (~ 1000 \$ per gram), thus creating significant barriers that prevent the utilization of LIBs in the wearable devices.

Flexible LIBs can be also produced by the micro-electromechanical systems (MEMS) fabrication technique in which the battery active materials are deposited on a flexible substrate in sequence (e.g., in cathode-electrolyte-anode sequence).^{13,14} As an example, Su et al. demonstrated a flexible LIB fabricated by a sequential deposition of a LiMnO_2 cathode layer, a LiPON electrolyte layer and a Li anode layer on a $70 \mu\text{m}$ thick stainless steel substrate using the RF sputtering technique.¹³ The as-fabricated LIB had a capacity of $12.8 \mu\text{Ah}$ when discharged at a current density of $5 \mu\text{A}/\text{cm}^2$. Also based on the MEMS fabrication technique, Vieira et al. reported fabrication of a flexible LIB that used Ge as anode, LiCoO_2

as cathode and LiPON as solid-state electrolyte.¹⁴ During the fabrication process, Si₃N₄ and LiPO thin layers were also deposited onto the cathode and anode respectively to provide electrical insulation and a battery chemical stability safeguard. The battery had a capacity of ~46 nAh/cm². We note that in a MEMS fabrication process, expensive deposition equipments such as RF-sputtering systems are generally required in order to have precise control of the coated battery layer.

In this paper, we report a flexible lithium-ion battery using graphite-paper (GP) with enhanced conductivity as current collectors (Fig. 1b). The enhancement of conductivity of GP was achieved by depositing a sub-micron thick metal layer onto a commercial graphite paper by physical vapor deposition (PVD). Particularly, we use an Al-deposited GP as the current collector for cathode and a bare GP or a copper-deposited GP as the current collector for anode. In this LIB, LiFePO₄ (LFP) and Li₄Ti₅O₁₂ (LTO) are used as cathode and anode active materials, and a polyethylene (PE) nanostructured membrane is used as a separator.

2 Experimental

2.1 Chemicals and materials

LiFePO₄, Li₄Ti₅O₁₂ and PE membranes were purchased from Targray Technology International Inc; Graphite papers (> 99%; thickness: ~25 μm) were purchased from Suzhou Dasen Electronic; Multi-walled carbon nanotubes (MWCNTs) and copper powder (> 99.7%) were obtained from Sigma-Aldrich. Al pellets (99.99%) are obtained from Kurt J. Lesker.

2.2 Battery sample fabrication

A highly conductive and flexible current collector was fabricated by depositing a sub-micron

thick aluminum or copper layer onto a graphite sheet by PVD (evaporative deposition, Edwards High Vacuum Ltd.). The PVD was performed under a high vacuum condition ($\sim 10^{-7}$ mbar) with a deposition rate of 0.2 nm/s. Then, the graphite sheet with a metallic coating was stored in N_2 -filled glove box for subsequent procedures. The obtained conductivity-enhanced GP (abbreviated as Al@GP in the following) current collector can be then used as substrates for deposition of LFP/PVDF to make LFP-Al@GP electrodes.

To synthesize the anode and cathode, LFP and LTO were first pre-mixed with MWCNT in a mortar, respectively. Then mixture was then dispersed in polyvinylidene fluoride (PVDF)/1-methyl-2-pyrrolidone solution using a magnetic stirrer for 4 h. The optimal weight ratio of LFP (or LTO), MWCNT and PVDF was found to be 8:1:1. The obtained slurry was then poured onto the current collector and made into a uniform wet-film using a Micrometer Adjustable Film Applicator (MTI Cooperation). The composites were dried in a vacuum furnace at 80 °C for 3 h, and then cut into 2*2 cm² square-shaped electrodes. These electrodes were then further dried at 110 °C for 12 h to ensure that the solvent (1-methyl-2-pyrrolidone) in slurry was completely evaporated.

The lithium-ion batteries were finally assembled by stacking the as-prepared electrodes together with a PE separator layer. 3 droplets (~ 0.15 mL) of electrolyte (1.0 M $LiPF_6$) dissolved in ethylene carbonate/dimethyl carbonate (EC/DEC) = 50/50 (v/v) from Sigma-Aldrich were added to the battery during the stacking process. Note that the battery assembly process was completed in a N_2 -filled glove box to avoid oxidation of electrolyte.

Finally, the battery was encapsulated with PE films using a lamination machine before it was taken out for characterization.

2.3 Characterization

The image of the cross section of the battery sample was taken by an optical microscope (Fig. 2a). The tomography of the Al coating on graphite paper substrate was investigated by scanning electron microscopy, and an energy dispersive spectrum (EDS) of the Al@GP was measured (Fig. 2b). The charge/discharge tests and EIS measurements were performed by an IviumStat.XR Electrochemical Work Station. All of the capacities and C-rate currents in this work were calculated based on the mass of LFP active materials (1 C corresponding to 170 mAh/g).

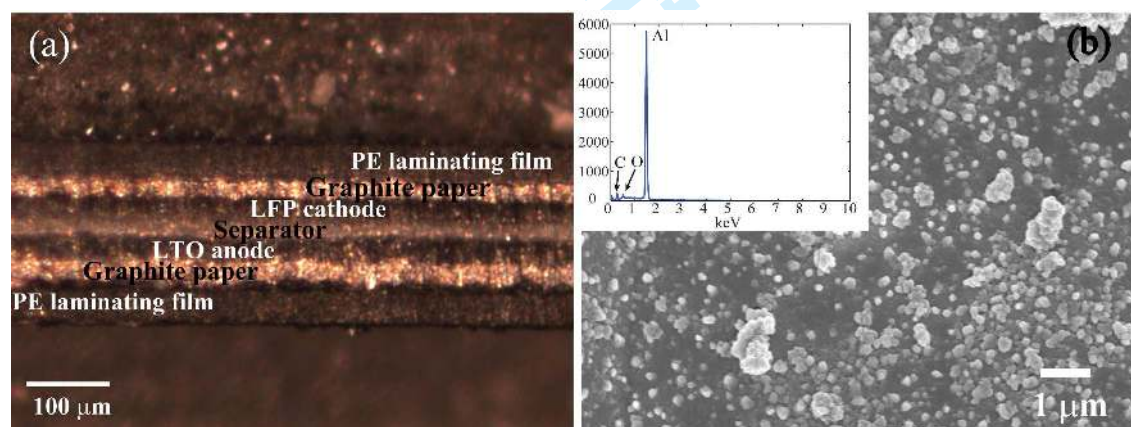


Fig. 2 (a) Cross section of the lithium-ion battery sample taken by an optical microscope; (b) SEM image of the Al coating on the graphite substrate and the inset is an energy dispersive spectrum (EDS) of the Al coating on the graphite paper.

3 Results and Discussion

3.1 Tomography and EDS of Al@GP

The tomography of Al@GP was studied by scanning electron microscopy. As shown in Fig. 2b, Al particles could aggregate to form clusters with the size ranging from tens to hundreds of microns, thus leading to a high aspect ratio and large activated surface area of the electrode. The EDS result suggests a good purity of the Al coating. The existence of oxygen is due to the passivation of the Al coating. The passivation layer is generally 2-5 nm thick and would not affect the electrochemical properties of the fabricated electrode.¹⁵

3.2 Electrochemical performance of the LFP/Al@GP electrode.

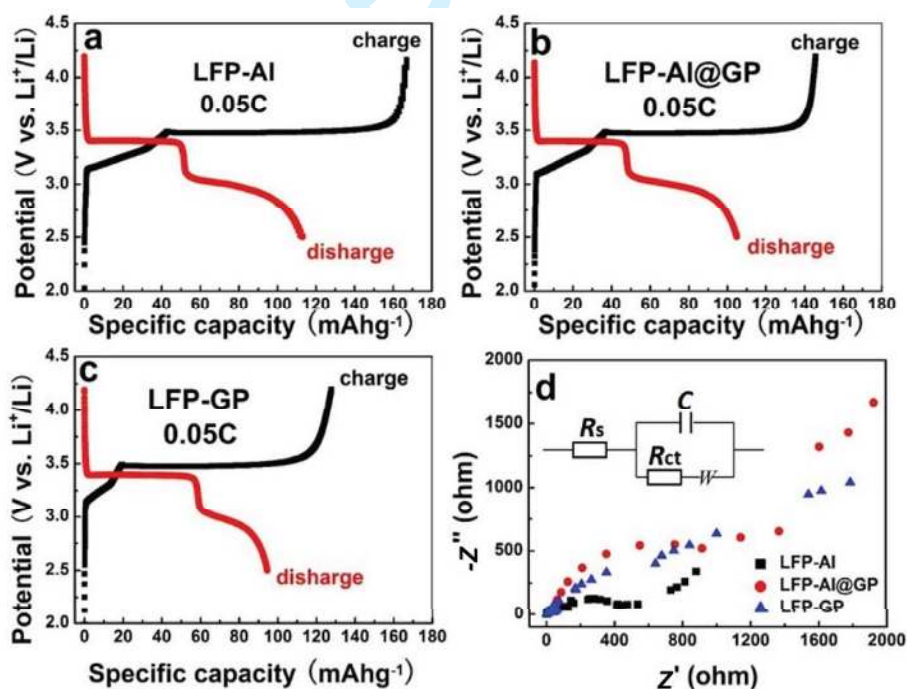


Fig. 3 charge/discharge voltage curves of the half cells with the rate of 0.05 C. (a) LFP-Al (foil), (b) LFP-Al@GP (Al enhanced GP), and (c) LFP-GP (pure GP). (d) Equivalent circuit and electrochemical impedance spectra of the LFP-Al@GP electrode, LFP-Al@GP electrode and a reference LFP-Al current

collector.

The electrochemical performance of the LFP-Al@GP electrode was characterized by the galvanostatic charge-discharge tests and EIS measurements. A half-cell battery with an active area of $2 \times 2 \text{ cm}^2$ was fabricated using LFP-Al@GP as the cathode and pure GP as the anode. The performance of this half-cell battery was compared with its two counterparts in which the cathode was fabricated by coating LFP onto an Al foil current collector (abbreviated as LFP-Al) or by coating LFP onto a GP current collector (abbreviated as LFP-GP). Note that the anode of reference half-cell batteries was also a $2 \times 2 \text{ cm}^2$ sized GP, the same as used in the LFP-Al@GP battery. The lithium-ion insertion/extraction properties of the LFP-Al cathode and LFP-Al@GP cathode were investigated by galvanostatic charge-discharge measurements. Fig. 3 represents the voltage curves in the first cycle of the charge/discharge test for batteries using the LFP-Al (Fig. 3a), LFP-Al@GP (Fig. 3b) and LFP-GP (Fig. 3c) with a 0.05 C charge/discharge rate. All the half-cells feature a $\sim 3.2 \text{ V}$ open circuit voltage. The capacity of the LFP-Al@GP//GP cell at 0.05 C discharge rate was 104.8 mAh/g with a coulombic efficiency of 71% (Fig. 3a). This was comparable to the performance of the half-cell battery using LFP-Al cathode that had a capacity of 113 mAh/g and a coulombic efficiency of 67.7% (see Fig. 3b). These results indicated that the Al@GP could be an excellent current collector for the cathode as its electrochemical properties are virtually identical to pure Al foil electrodes. Besides, we also investigated how thickness of the coated aluminum current collector would affect the performance of the half-cell battery. Experimentally, we fabricated several LFP-Al@GP cells with the thickness of coated aluminum layers ranging from 50 nm

to 200 nm with a 50 nm step. As a matter of fact, these LFP-Al@GP cells show virtually identical performances in the charge-discharge measurements. We, therefore, conclude that the thickness of the aluminum layer has an insignificant effect on the electrochemical properties of the LFP-Al@GP electrode.

To investigate the conductivity of a cathode, EIS measurements of LFP-Al@GP were performed, and the results were compared to those of LFP-Al and LFP-GP. Fig. 3d shows the Nyquist plots of the fresh LFP-Al//GP, LFP-Al@GP//GP, and LFP-GP//GP half-cells after the first 0.2 C charge-discharge cycle. Nyquist plots are composed of a depressed semicircle in the high-to-medium frequency region together with a slope in the low frequency region. According to the order of decreasing frequency, the EIS spectra can be divided into three distinct regions. The first intercept on the real axis in Fig. 3d (high frequency region) gives the equivalent series resistance (ESR), R_s , which is a bulk electrolyte resistance. The second intercept (lower frequency region) gives a sum of the electrolyte resistance, R_s , and the charge transfer resistance, R_{ct} , which is the electrode/electrolyte interfacial resistance.¹⁶ The values of the charge-transfer resistance R_{ct} of the LFP-Al@GP electrode was 920 Ω , which are higher than that of the LFP-Al ($R_{ct} = 400 \Omega$), but is significantly lower than that of the LFP-GP. Note that the Al@GP is much more flexible and lighter compared to a pure Al foil. All these results indicated that the Al@GP fabricated by PVD method, could be an excellent candidate of current collector for highly flexible LIBs. However, it is meaningless to discuss more of the batteries' performance when GP was used directly as the anode without any modification or improvements.

It is worth to note that that, if a GP is directly used as a current collector, coating of the battery active materials onto a pure GP is challenging, since the coated layer tends to peel off. Thus, yield of the corresponding electrodes is less than 10 %. However, yield of the electrodes can experimentally reach almost 100%, if electrodes are made from a GP enhanced with a sub-micron thick metal layer. Therefore, depositing a submicron thick layer onto a GP not only enhances the conductivity of the current collector, but also mechanically improves the adhesion between the battery active materials and the current collector, thus facilitating the subsequent battery assembly process and its reliability.

3.3 Assembly and Electrochemical Behavior of the LFP-Al@GP//LTO-GP Flexible full Battery

Since LFP and LTO have the well-matched theoretical capacities of 170 mAh/g and 175 mAh/g, and the LFP/Al@GP electrode showed excellent electrochemical performance that is comparable to that of LFP -Al, we proceeded with a full battery assembly. We fabricated a thin, and flexible LFP-Al@GP//LTO-GP full battery using the flexible LFP-Al@GP cathode and the LTO-GP anode.

To assemble a full battery, the integrated cathode was first attached to the sticky side of a polyethylene (PE) lamination film. Then we stacked the PE separator on top of the cathode, and added three droplets of LiPF_6 electrolyte. The counter electrode and another PE lamination film were then stacked to the battery structure one after another. Finally, the full battery was then encapsulated using a laminating machine. All of these assembly processes

were carried out in a N₂-filled glove box.

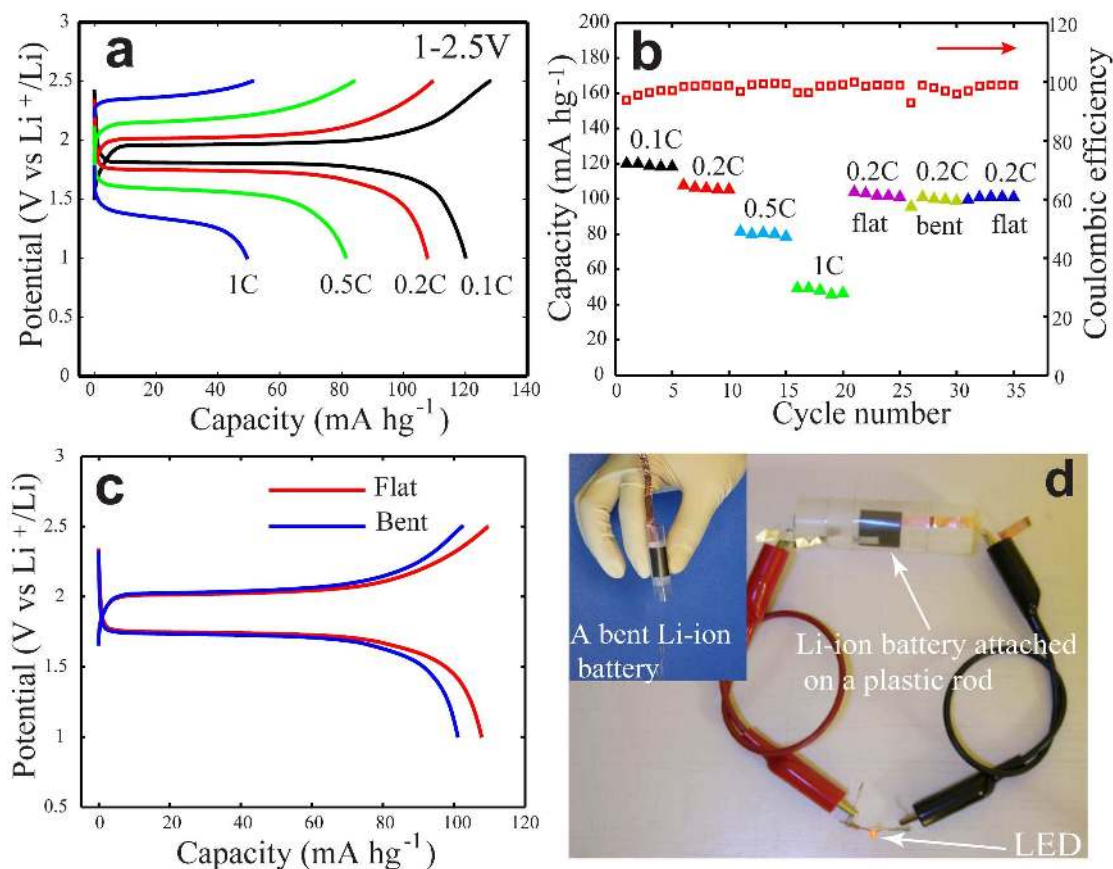


Fig. 4 Characterization of the LFP-Al@GP//LTO-GP full battery. (a) Charge/discharge voltage curves of the battery with different charge-discharge rates. (b) Capacity and coulombic efficiency of the battery with different charge-discharge rates for 35 cycles. (c) Voltage curves of the flat battery (red line) and a bent battery (blue line). The bending radius of the battery is ~ 1 cm. (d) A LED was lit up by a bent full battery. The inset demonstrates the excellent flexibility of the full battery.

The electrochemical properties of a full battery were investigated using charge /discharge cyclic analysis with different charge/discharge rates (from 0.1 C to 1 C) as shown in Fig. 4a.

Consistent with the theoretical value of a LFP-LTO battery, the operating voltage of this full battery was found to be ~ 1.9 V. As shown in Fig. 4a and b, the LFP-Al@GP//LTO-GP battery had an excellent rate capacity, which was calculated to be 120.2, 107.8, 81.8 and 49.4 mAhg⁻¹ at 0.1, 0.2, 0.5, and 1 C, respectively. It can be clearly seen that the discharge capacities exhibit a tendency to decrease with the increment of current density; however, the voltage plateau still remained flat even when current density is up to 1 C, indicating an excellent charge/discharge performance. Moreover, after a series of tests under different charge/discharge rates, the discharge capacity of the battery was still as high as 103.8 mAhg⁻¹, when the rate turned back to 0.2 C. This suggests that the structure of each components of the full battery remained intact after subjecting to high current densities. The coulombic efficiencies of the full battery were $> 94\%$ during the whole cycle.

Due to the small thickness and high flexibility of the metal-enhanced GP current collectors and the as-integrated LFP-Al@GP and LTO-GP electrodes, the full battery shows excellent flexibility. The effect of bending on the performance of the flexible battery was also investigated. Fig. 4c shows the charge/discharge measurement of the bent battery at 0.2 C after 25 charge/discharge cycles under different rates. Compared with the flat state, only a slight overpotential was observed, and a 2% decrease in capacity was found. What's more, the flexible battery showed an excellent cyclic stability both under flat and bent states (see Fig. 4b and c). The retention capacity of the bent battery was $\sim 92\%$ of that of the flat battery even after the battery undergoes 25 charge/discharge cycles. Furthermore, we note that even after bending the battery for another 5 charge/discharge cycles, more than 93% of the

capacity could be still restored if the battery is released. In Fig. 4d, we demonstrate that a LED could be lit up by the battery bent at a 1 cm radius.

Conclusions

In summary, an ultra-thin flexible battery with total thickness of less than 250 μm was successfully fabricated by using conductivity-enhanced metal-deposited GP current collector. To fabricate this highly flexible and conductive current collector, we deposit sub-micron thick metallic layers onto the GP using PVD technique. Compared to traditional current collectors based on pure metal (such as Al or Cu) foils, the proposed current collector is advantageous due to its light weight, high flexibility and improved surface adhesion for depositing battery electrode materials. The battery uses LiFePO_4 and $\text{Li}_4\text{Ti}_5\text{O}_{12}$ as the cathode and anode materials, and PE membrane soaked in LiPF_6 as a separator. The battery could achieve a rate capacity of $\sim 100 \text{ mAhg}^{-1}$ under standard 0.2 C charge/discharge rate. Besides, the battery could retain its capacity even after intensive cyclic charge/discharge operation. During all the battery operation, the coulombic efficiency of the battery remains above 94%. We believe that this battery could find its niche markets in numerous fields relevant to portable or wearable electronic devices.

References

- (1) Gwon, H.; Hong, J.; Kim, H.; Seo, D.-H.; Jeon, S.; Kang, K. *Energy & Environmental Science* **2014**, *7*, 538.
- (2) Zhou, G.; Li, F.; Cheng, H.-M. *Energy & Environmental Science* **2014**, *7*, 1307.
- (3) Armand, M.; Tarascon, J.-M. *Nature* **2008**, *451*, 652.
- (4) Li, N.; Chen, Z.; Ren, W.; Li, F.; Cheng, H.-M. *Proceedings of the National Academy of Sciences* **2012**, *109*, 17360.

- (5) Koo, M.; Park, K.-I.; Lee, S. H.; Suh, M.; Jeon, D. Y.; Choi, J. W.; Kang, K.; Lee, K. J. *Nano letters* **2012**, *12*, 4810.
- (6) Vlad, A.; Reddy, A. L. M.; Ajayan, A.; Singh, N.; Gohy, J.-F.; Melinte, S.; Ajayan, P. M. *Proceedings of the National Academy of Sciences* **2012**, *109*, 15168.
- (7) Wei, D.; Haque, S.; Andrew, P.; Kivioja, J.; Ryhänen, T.; Pesquera, A.; Centeno, A.; Alonso, B.; Chuvilin, A.; Zurutuza, A. *Journal of Materials Chemistry A* **2013**, *1*, 3177.
- (8) Liu, Y.; Gorgutsa, S.; Santato, C.; Skorobogatiy, M. *Journal of the Electrochemical Society* **2012**, *159*, A349.
- (9) Wang, K.; Luo, S.; Wu, Y.; He, X.; Zhao, F.; Wang, J.; Jiang, K.; Fan, S. *Advanced Functional Materials* **2013**, *23*, 846.
- (10) Li, X.; Yang, J.; Hu, Y.; Wang, J.; Li, Y.; Cai, M.; Li, R.; Sun, X. *Journal of Materials Chemistry* **2012**, *22*, 18847.
- (11) Hu, Y.; Li, X.; Wang, J.; Li, R.; Sun, X. *Journal of Power Sources* **2013**, *237*, 41.
- (12) Yoon, S.; Lee, S.; Kim, S.; Park, K.-W.; Cho, D.; Jeong, Y. *Journal of Power Sources* **2015**, *279*, 495.
- (13) Su, C.-H.; Hsueh, T.-H.; Jheng, Y.-R.; Yu, Y.-J.; Jan, D.-J.; Wang, M.-C. *ECS Transactions* **2014**, *59*, 103.
- (14) Vieira, E.; Ribeiro, J.; Sousa, R.; Correia, J.; Goncalves, L. *Journal of Micromechanics and Microengineering* **2016**, *26*, 084002.
- (15) Evertsson, J.; Bertram, F.; Zhang, F.; Rullik, L.; Merte, L.; Shipilin, M.; Soldemo, M.; Ahmadi, S.; Vinogradov, N.; Carlà, F. *Applied surface science* **2015**, *349*, 826.
- (16) Rakhi, R.; Chen, W.; Cha, D.; Alshareef, H. *Nano letters* **2012**, *12*, 2559.

Figure captions

Fig.1 (a) Schematic of the thin, flexible lithium-ion battery, and (b) a lithium-ion battery sample

Fig.2 (a) Cross section of the lithium-ion battery sample taken by an optical microscope; (b) SEM image of the Al coating on the graphite paper substrate and the inset is an energy dispersive spectrum (EDS) of the Al coating on the graphite paper.

Fig. 3 charge/discharge voltage curves of the half cells with rate of 0.05 C. (a) LFP-Al (foil), (b) LFP-Al@GP (Al enhanced GP), and (c) LFP-GP (pure GP). (d) Equivalent circuit and electrochemical impedance spectra of the LFP-Al@GP electrode, LFP-Al@GP electrode and a reference LFP-Al current collector.

Fig. 4 Characterization of the LFP-Al@GP//LTO-GP full battery. (a) Charge/discharge voltage curves of the battery with different charge-discharge rates. (b) Capacity and coulombic efficiency of the battery with different charge-discharge rates for 35 cycles. (c) Voltage curves of the flat battery (red line) and a bent battery (blue line). The bending radius of the battery is ~1 cm. (d) A LED was lit up by a bent full battery. The inset demonstrates the excellent flexibility of the full battery.